

The U-box ubiquitin ligase TUD1 promotes brassinosteroid-induced GSK2 degradation in rice

Dapu Liu^{1,4}, Xiaoxing Zhang^{1,4}, Qingliang Li², Yunhua Xiao², Guoxia Zhang², Wenchao Yin¹, Mei Niu¹, Wenjing Meng¹, Nana Dong¹, Jihong Liu¹, Yanzhao Yang¹, Qi Xie², Chengcai Chu² and Hongning Tong^{1,3,*}

¹National Key Facility for Crop Gene Resources and Genetic Improvement, Institute of Crop Sciences, Chinese Academy of Agricultural Sciences, Beijing 100081, China

²State Key Laboratory of Plant Genomics, Institute of Genetics and Developmental Biology, The Innovative Academy for Seed Design, Chinese Academy of Sciences, Beijing 100101, China

³National Nanfan Research Institute, Chinese Academy of Agricultural Sciences, Sanya 572024, China

⁴These authors contributed equally to this article.

*Correspondence: Hongning Tong (tonghongning@caas.cn)

<https://doi.org/10.1016/j.xplc.2022.100450>

ABSTRACT

Brassinosteroids (BRs) are a class of steroid hormones with great potential for use in crop improvement. De-repression is usually one of the key events in hormone signaling. However, how the stability of GSK2, the central negative regulator of BR signaling in rice (*Oryza sativa*), is regulated by BRs remains elusive. Here, we identify the U-box ubiquitin ligase TUD1 as a GSK2-interacting protein by yeast two-hybrid screening. We show that TUD1 is able to directly interact with GSK2 and ubiquitinate the protein. Phenotypes of the *tud1* mutant are highly similar to those of plants with constitutively activated GSK2. Consistent with this finding, GSK2 protein accumulates in the *tud1* mutant compared with the wild type. In addition, inhibition of BR synthesis promotes GSK2 accumulation and suppresses TUD1 stability. By contrast, BRs can induce GSK2 degradation but promote TUD1 accumulation. Furthermore, the GSK2 degradation process is largely impaired in *tud1* in response to BR. In conclusion, our study demonstrates the role of TUD1 in BR-induced GSK2 degradation, thereby advancing our understanding of a critical step in the BR signaling pathway of rice.

Key words: brassinosteroid, TUD1, GSK2, signal transduction, ubiquitination

Liu D., Zhang X., Li Q., Xiao Y., Zhang G., Yin W., Niu M., Meng W., Dong N., Liu J., Yang Y., Xie Q., Chu C., and Tong H. (2023). The U-box ubiquitin ligase TUD1 promotes brassinosteroid-induced GSK2 degradation in rice. *Plant Comm.* 4, 100450.

INTRODUCTION

Brassinosteroids (BRs) are a class of steroid hormones that play important roles in diverse aspects of plant growth and development. Since the identification of the first BR in the late 1970s (Grove et al., 1979), our understanding of BR synthesis and signaling has progressed rapidly, particularly in the model plant *Arabidopsis* (*Arabidopsis thaliana*). BRs are perceived by a membrane receptor complex, and their recognition stimulates a series of phosphorylation and dephosphorylation events involving multiple protein families (Nolan et al., 2020). Representative members of this primary BR signaling pathway include BRI1 receptor kinase (Wang et al., 2001), BAK1 co-receptor kinase (Li et al., 2002; Nam and Li, 2002), BSK1 kinase (Tang et al., 2008), CDG1 kinase (Kim et al., 2011), BSU1 phosphatase (Mora-Garcia et al., 2004), BIN2 kinase (Li and Nam, 2002), PP2A phosphatase (Tang et al., 2011; Wu et al.,

2011), and BZR1/BES1 transcription factors (He et al., 2002; Yin et al., 2002). Among them, BIN2 and its several homologs, members of the GSK3-like kinase family, are central negative regulators of BR signaling. BRs must destabilize BIN2 to release BZR1/BES1 to activate BR responses. Certain mutations in *bin2-D* mutants confer enhanced BIN2 stability, resulting in strong BR-insensitive phenotypes (Li and Nam, 2002; Peng et al., 2008). Regulation of BIN2 stability is mediated by the F-box E3 ubiquitin ligase KIB1, which interacts with BIN2 and promotes BIN2 ubiquitination and degradation (Zhu et al., 2017). Co-suppression of *KIB1* and its homologous genes leads to BIN2 accumulation and thus to phenotypes similar to *bin2-D* (Zhu et al., 2017).

Published by the Plant Communications Shanghai Editorial Office in association with Cell Press, an imprint of Elsevier Inc., on behalf of CSPB and CEMPS, CAS.

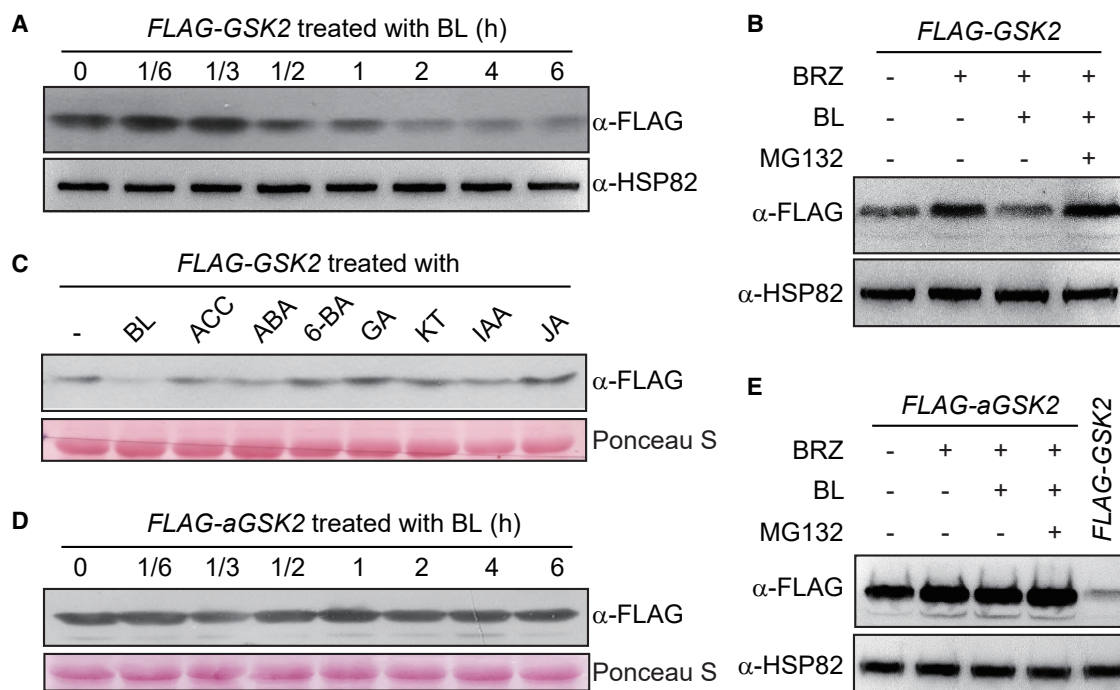


Figure 1. BRs induce GSK2 degradation through the 26S proteasome.

(A) Effect of BL on GSK2. One-week-old *FLAG-GSK2* seedlings were treated with 1 μ M BL for different times. HSP82 was detected as a control.
(B) Effect of BL, BRZ, and MG132 on GSK2. One-week-old seedlings were treated with different combinations of 1 μ M BL, 10 μ M BRZ, and 20 μ M MG132 for 6 h. HSP82 was detected as a control.
(C) Effect of different hormones on GSK2. One-week-old seedlings were treated with different chemicals (1 μ M, 6 h). ACC, 1-aminocyclopropane-1-carboxylic acid; ABA, abscisic acid; 6-BA, 6-benzylaminopurine; GA, gibberellic acid; KT, kinetin; IAA, indole-3-acetic acid; JA, jasmonic acid. Staining with Ponceau S is shown as a loading control.
(D) Effect of BL on *aGSK2*. One-week-old *Flag-aGSK2* seedlings were treated with 1 μ M BL. Staining with Ponceau S is shown as a loading control.
(E) Effect of BL, BRZ, and MG132 on *aGSK2*. One-week-old seedlings were treated with different combinations of 1 μ M BL, 10 μ M BRZ, and 20 μ M MG132 for 6 h. HSP82 was detected as a control.

Rice (*Oryza sativa*), as a crop plant, feeds more than half of the world's population. BRs regulate many important agronomic traits in rice, such as plant height, leaf angle, and grain size (Tong and Chu, 2018). BRs also regulate plant responses to various biotic and abiotic stresses (Tong and Chu, 2018). Thus, elucidation of BR signaling in rice is important for the utilization of BR genes for crop improvement. A number of orthologs of the above-mentioned BR signaling components have been identified in rice, such as OsBRI1 (Yamamoto et al., 2000), OsBAK1 (Li et al., 2009), OsBSK3 (Zhang et al., 2015), GSK2 (OsBIN2) (Tong et al., 2012), and OsBZR1 (Bai et al., 2007). Extensive genetic studies involving mutants and transgenic analyses have suggested the existence of a conserved BR signaling pathway in rice (Liu et al., 2021). Although overexpression of wild-type GSK2 failed to produce obvious phenotypes, overexpression of a mutant GSK2 mimic of *bin2-D* led to strong BR-insensitive phenotypes, including severely dwarfed stature, compact architecture, twisted leaves, and reduced grain size (Tong et al., 2012). By contrast, simultaneous knockout of GSK2 and its homologous genes resulted in enhanced BR signaling, enlarged leaf angles, and increased grain size (Liu et al., 2021). Although these results suggest a critical negative role for GSK2 in BR signaling, how GSK2 stability is regulated in rice remains elusive.

Here, we identified the U-box ubiquitin ligase TUD1 as a GSK2-interacting protein. TUD1, also named ELF1/DSG1/D1352/PUB26,

has been shown to participate in BR signaling by several different groups (Hu et al., 2013; Sakamoto et al., 2013; Ren et al., 2014; Wang et al., 2017). However, the underlying mechanism by which TUD1 regulates BR signaling remains largely unclear. We found that phenotypes of *tud1* mutants are highly similar to those of GSK2-activated plants, and we demonstrated that TUD1 promotes GSK2 ubiquitination and degradation in response to BRs.

RESULTS

BRs induce GSK2 degradation through the 26S proteasome

We have generated a number of *FLAG-GSK2* transgenic lines (Liu et al., 2021), and we identified one with moderate expression of the fusion protein that could be suitable for the study of GSK2 regulation. When the plants were treated with brassinolide (BL, 1 μ M), one of the active BRs, *FLAG-GSK2* levels were significantly decreased in half an hour and became much lower in 2–6 hours (Figure 1A). By contrast, when the plants were treated with brassinazole (BRZ, 10 μ M, 6 h), a specific inhibitor of BR synthesis, *FLAG-GSK2* accumulated significantly (Figure 1B). Compared with BRZ alone, a combination of BRZ and BL greatly induced protein degradation (Figure 1B). However, BL failed to induce protein

degradation in the presence of MG132 (20 μ M), an inhibitor of the 26S proteasome (Figure 1B).

We evaluated the effect of various phytohormones on GSK2 stability, and we found that BL had a more severe effect on GSK2 abundance than any of the other hormones (Figure 1C). It has been shown that the stabilized form of BIN2 in the gain-of-function *bin2-1* mutant is unresponsive to BL application (Peng et al., 2008). To test whether the mutation confers a similar effect on GSK2, we generated transgenic plants overexpressing the activated GSK2 (aGSK2) mimic of the BIN2-1 mutation fused with a FLAG tag. Similar to BIN2-1 in *Arabidopsis* (Peng et al., 2008), FLAG-aGSK2 had basically no response to BL, even after a 6-h treatment (Figure 1D). In addition, treatment with BRZ, BRZ plus BL, or BRZ plus both BL and MG132 also had no clear effect on FLAG-aGSK2 abundance (Figure 1E). Taken together, these results suggested that BRs induce GSK2 degradation through the 26S proteasome, and FLAG-GSK2 plants could serve as suitable materials for the investigation of GSK2 stability regulated by BRs.

GSK2 interacts with TUD1 *in vivo* and *in vitro*

We identified TUD1 as a potential GSK2-interacting protein through large-scale yeast two-hybrid screening. TUD1 is a U-box ubiquitin ligase (Hu et al., 2013) and may therefore be involved in GSK2 degradation. The interaction of this specific protein pair was first confirmed by yeast two-hybrid analysis using GSK2 as bait and full-length TUD1 (459 amino acids, aa) as prey (Figure 2A). In addition, aGSK2 also interacted with TUD1 in the analysis (Figure 2A). We truncated TUD1 into segments of different lengths, and we determined that the interaction requires the N-terminal region (1–250 aa) that contains the U-box domain (Supplemental Figure 1). A further *in vitro* test using recombinant proteins revealed that TUD1 tagged with MBP (maltose binding protein) can easily be pulled down by GSK2 tagged with GST (glutathione S-transferase) but not by GST alone (Figure 2B). The interaction was also verified by a split-luciferase complementation assay (Figure 2C). GSK2 and TUD1 were fused with the two parts of luciferase, respectively. When the two chimeric proteins were co-expressed in *Nicotiana benthamiana* leaves, luciferase activity was reconstituted through the association of GSK2 with TUD1 (Figure 2C). In co-immunoprecipitation (Co-IP) analysis, both GFP-TUD1 and FLAG-GSK2 could be detected in the compound isolated using anti-GFP antibody (Figure 2D). As a negative control, substitution of GFP alone for GFP-TUD1 failed to pull down FLAG-GSK2 (Figure 2D). These results demonstrated that GSK2 physically interacts with TUD1 *in vivo* and *in vitro*.

Spatial overlap and specific interaction between TUD1 and GSK2

Spatial overlap could be a prerequisite for the protein–protein interaction. At the transcriptional level, both *TUD1* and *GSK2* were expressed in various tissues according to a public gene expression database (Supplemental Figure 2; <http://ricexpro.dna.affrc.go.jp/>). At the cellular level, the localization patterns of GFP-TUD1 and GSK2-GFP appeared to be highly similar; both showed ubiquitous localization, as evaluated by fluorescence microscopy observation of rice protoplasts (Supplemental Figure 3).

To confirm this result, we performed bimolecular fluorescence complementation (BiFC) analysis. Indeed, the interaction signal between GSK2 and TUD1, as well as between aGSK2 and TUD1, had a distribution pattern similar to those of GFP-TUD1 or GSK2-GFP (Figure 2E). GSK2 belongs to a specific clade of the GSK3-like kinase family. In rice, this clade contains four members, GSK1–GSK4, which have been suggested to redundantly regulate BR signaling (Liu et al., 2021). Unexpectedly, yeast two-hybrid analysis revealed that TUD1 did not interact with GSK3 or GSK4 and interacted very weakly with GSK1 (Figure 2F). Although the specific interaction with GSK2 requires further verification, it implies that the TUD1-GSK2 module may play a distinctive role in rice BR signaling. Taken together, these analyses corroborated the interaction between GSK2 and TUD1.

Strong resemblance between *tud1* mutant and aGSK2-overexpressing plants

Next, we sought genetic evidence by comparing the characteristics of GSK2- and TUD1-related plants. *Go-3* is one of the severe lines overexpressing aGSK2 in the Zhonghua11 (ZH11, a *japonica* variety) background (Tong et al., 2012). *tud1-5* is a loss-of-function mutant in the Nipponbare (NP, a *japonica* variety) background (Hu et al., 2013). According to previous reports as well as our observations here, the phenotypes of the two plants are highly similar, basically the same as each other (Figure 3A). Both plants exhibited an extremely dwarfed stature with a compact architecture and dark-green leaves (Figure 3A). In addition, both plants developed twisted and wrinkled leaves (Figure 3B), a feature of BR-deficient mutants (Tong et al., 2012). Moreover, both plants had reduced grain size, impaired BR sensitivity, and increased expression of BR biosynthetic genes (Tong et al., 2012; Hu et al., 2013; Ren et al., 2014; Wang et al., 2017). We also performed transcriptome analyses to globally evaluate the molecular changes in the two plants. For a better comparison in the same wild-type background, we produced a new *tud1* knockout allele in the ZH11 background by CRISPR-Cas9 genome editing; it contained a frame shift mutation in the *TUD1* coding sequence and showed phenotypes just like those of *tud1-5*. We identified 3324 differentially expressed genes (DEGs) between *Go-3* and ZH11 and 2210 DEGs between *tud1* and ZH11. Overlapping analysis revealed that 1346 DEGs were co-regulated in both *Go-3* and *tud1* (Supplemental Figure 4A). Among these, 93.7% (1261/1346) were regulated in a consistent direction, including 615 up- and 646 downregulated in both *Go-3* and *tud1* (Supplemental Figure 4B and 4C, Supplemental Dataset). Accordingly, six genes with annotations related to BR showed a consistent expression trend in *Go-3* and *tud1* (Supplemental Figure 4D). These analyses suggested that GSK2 and TUD1 co-regulate a large number of common genes. It is well known that the GSK3-like kinase GSK2 phosphorylates OsBZR1 to regulate BR signaling. We introduced TUD1 into protoplasts prepared from a GFP-Myc-OsBZR1 transgenic line (Liu et al., 2021) and found that the OsBZR1 fusion proteins, mostly in dephosphorylated forms, were accumulated at high levels (Supplemental Figure 5), demonstrating that TUD1, like GSK2, indeed regulates BR signaling. We also examined the cellular changes in *Go-3* and *tud1-5* using both leaf sheaths and grain husks (Figure 3C–3F). Compared with their respective wild types, *Go-3* and *tud1-5*

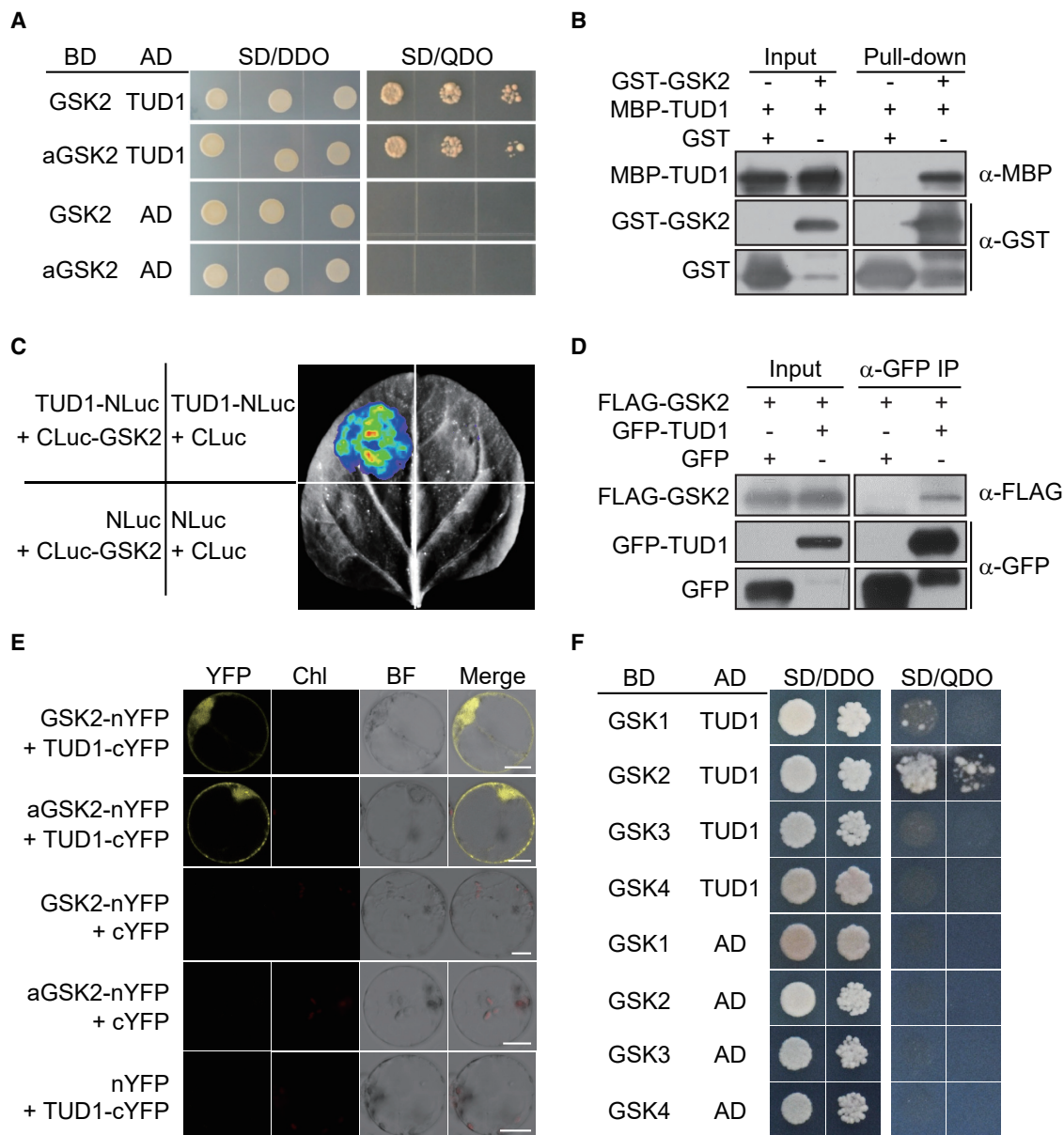


Figure 2. GSK2 interacts with TUD1 in vivo and in vitro.

(A) Yeast two-hybrid analysis of the interactions between GSK2/aGSK2 and TUD1. Yeast co-transformants were grown on selective dropout media. SD/DDO, double dropout without tryptophan and leucine. SD/QDO, quadruple dropout without tryptophan, leucine, histidine, and adenine.

(B) Pull-down assay of the interaction between GSK2 and TUD1. GST-beads were used for pull-down, and the resulting proteins were detected with anti-MBP (α-MBP) and α-GST antibodies.

(C) Luciferase complementation assay of the interaction between GSK2 and TUD1 performed in *N. benthamiana* leaves.

(D) Co-IP assay of the interaction between GSK2 and TUD1. Co-expressed FLAG-GSK2 and GFP-TUD1 were immunoprecipitated with α-GFP beads and then detected using α-FLAG antibody.

(E) BiFC assay showing the co-localization of GSK2/aGSK2 and TUD1 in protoplasts. Chl, chloroplast fluorescence; BF, bright field. Scale bars represent 10 μm.

(F) Yeast two-hybrid assay testing the interactions between GSK1/2/3/4 and TUD1. Yeast co-transformants with different combinations of the bait and prey proteins were grown on SD/DDO and SD/QDO for testing.

showed significant reductions in cell length in both tissues, and statistical analyses indicated that the extent of this reduction was similar in both genotypes (Figure 3C–3F). The strong resemblance between the two plants at the morphological, cellular, and molecular levels indicated the close functional association between TUD1 and GSK2 in BR signaling.

To further investigate the genetic relationship between TUD1 and GSK2, we crossed *tud1-5* with *Go-1*, a weak *Go* line (Tong et al., 2012), and generated their double mutant *Go-1 tud1-5*. Compared with *tud1-5*, *Go-1 tud1-5* showed a slight overall enhancement in the severity of the phenotypes (Figure 3G). However, statistical analyses of plant height and grain length

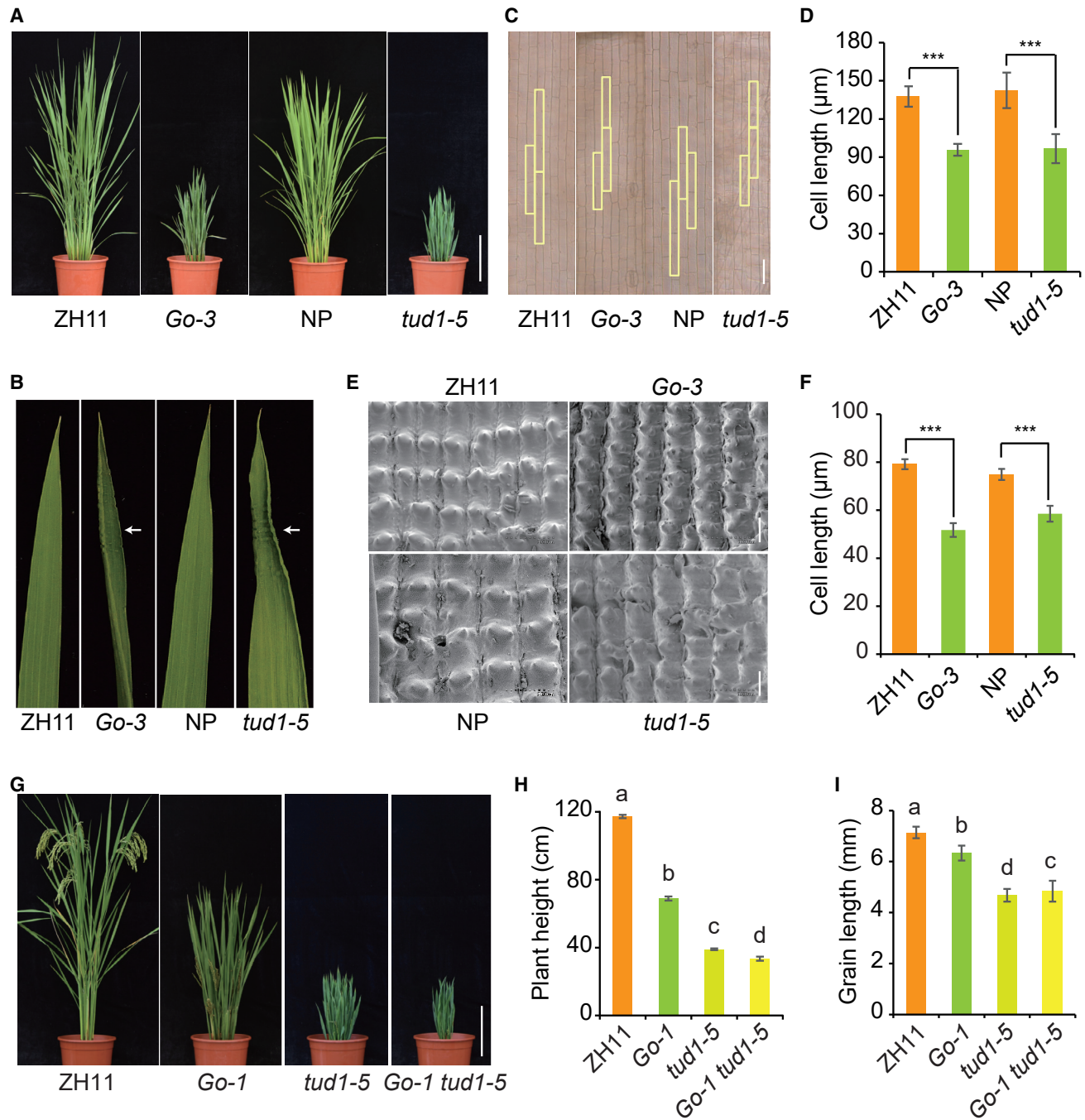


Figure 3. Resemblance between *tud1* and GSK2-activated plants.

(A) Gross morphology of *Go-3*, *tud1-5*, and their respective wild-type backgrounds. *Go-3* is a severe *aGSK2* transgenic line. Scale bar represents 20 cm.
 (B) Wrinkled leaves of the plants. Arrows indicate the wrinkled parts.
 (C) Longitudinal sections of the leaf sheath from 1-month-old seedlings of *tud1-5* and *Go-3*. Three cells in each sample are outlined for comparison. Scale bar represents 50 μm.
 (D) Statistical data for cell length ($n = 10$). Bars indicate standard deviation (SD), and $***P < 0.001$ by *t*-test.
 (E) Scanning microscopy observation of the outer surface of *tud1-5* and *Go-3* lemma. Scale bars represent 50 μm.
 (F) Statistical data for cell length ($n = 20$). Bars indicate SD, and $***P < 0.001$ by *t*-test.
 (G) Gross morphology of the plants for double mutant analysis. Scale bar represents 20 cm.
 (H) and (I) Statistical data for plant height (H, $n = 10$) and grain length (I, $n = 30$). Bars indicate SD. Letters on histograms indicate significant differences according to ANOVA followed by the least significant difference (LSD) test ($P < 0.05$).

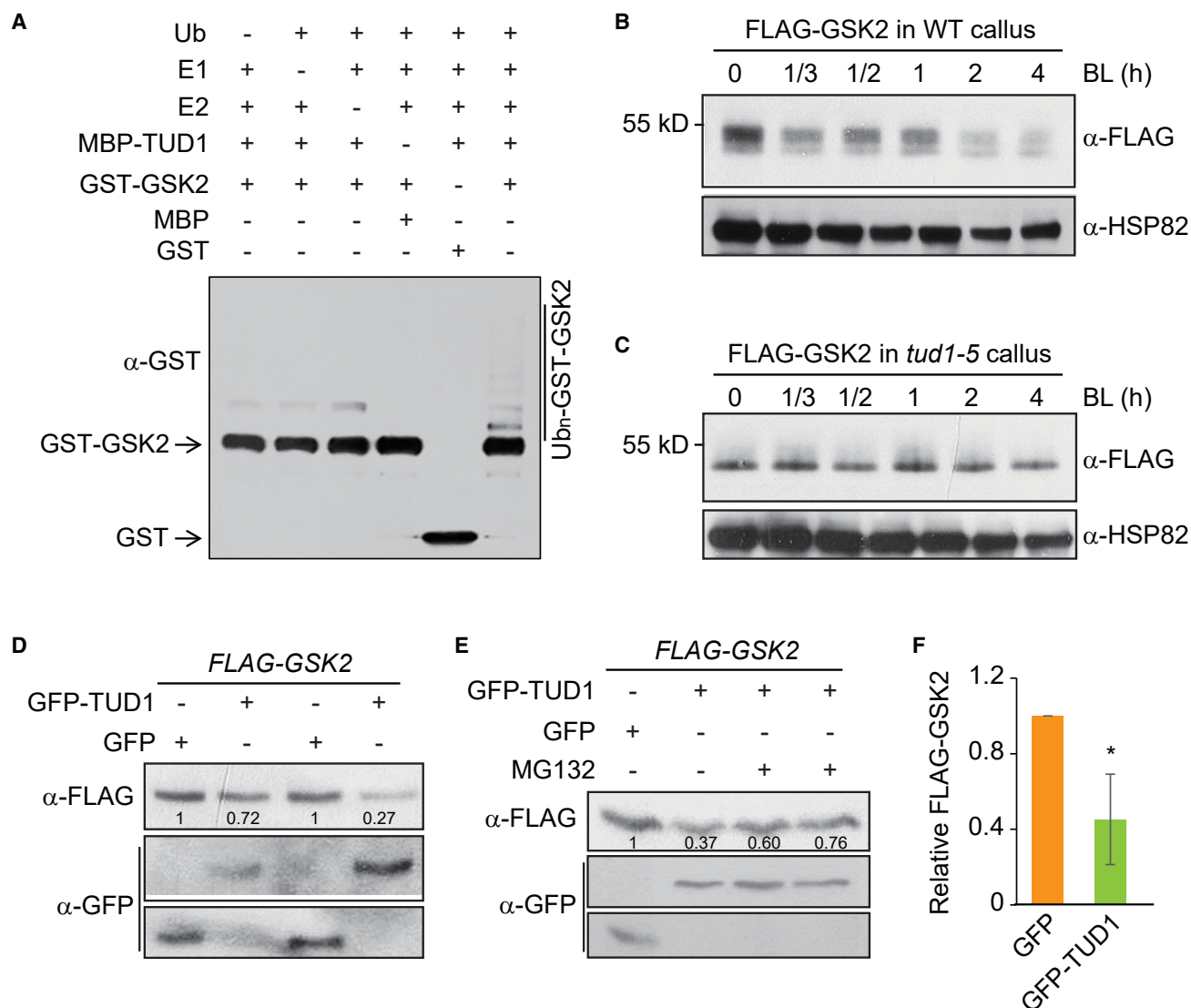


Figure 4. TUD1 promotes GSK2 ubiquitination and degradation.

(A) TUD1 mediates the ubiquitination of GSK2 *in vitro*. Mixtures with different combinations of proteins were incubated at 30°C for 90 min and then detected with α -GST antibody. The protein ladder corresponding to poly-ubiquitinated GST-GSK2 (Ub_n-GST-GSK2) is indicated.

(B) and (C) Effect of BL on GSK2 in wild-type (WT, B) and *tud1-5* (C) callus. Transfected callus expressing FLAG-GSK2 was treated with 1 μ M BL for different times. FLAG-GSK2 was detected using α -FLAG antibody, and HSP82 was detected as a control.

(D) Effect of TUD1 on GSK2 in rice protoplasts. Protoplasts isolated from FLAG-GSK2 seedlings were used to express GFP or GFP-TUD1. The gray values of the bands were quantified to determine the protein levels.

(E) Effect of MG132 on TUD1-promoted GSK2 degradation. Protoplasts expressing TUD1 and GSK2 were treated with 20 μ M MG132 for 1 h.

(F) Statistical data showing the effect of TUD1 on GSK2 protein levels ($n = 3$). Bars indicate SD, and * $P < 0.05$ by *t*-test.

indicated that the difference between *Go-1 tud1-5* and *tud1-5* was much smaller than that between *Go-1* and ZH11 (Figure 3H and 3I), indicating the existence of an epistatic interaction between GSK2 and TUD1. Considering that TUD1 encodes a ubiquitin ligase, this result strongly suggested that TUD1 functions by regulating GSK2 stability.

TUD1 promotes GSK2 ubiquitination and degradation

It has been demonstrated that TUD1 is a functional ubiquitin ligase (Hu et al., 2013). In an *in vitro* ubiquitination system, incubation of GSK2 and TUD1 in the presence of ubiquitin, E1,

and E2 resulted in a ladder of slower-shifted GSK2, corresponding to poly-ubiquitinated GSK2 forms (Figure 4A). As controls, removal of any of these components led to failure of the modification (Figure 4A). Therefore, TUD1 is directly involved in GSK2 ubiquitination. To test whether TUD1 is involved in BR-induced GSK2 instability, we introduced a construct expressing FLAG-GSK2 into wild-type and *tud1-5* callus, and we examined the effect of BR on the fusion protein (Figure 4B and 4C). Intriguingly, there were multiple migrating forms of FLAG-GSK2 in the callus, and the major form in the wild type appeared to be higher than that in the *tud1-5* mutant (Figure 4B and 4C). Nevertheless, BL treatment overall induced GSK2 degradation

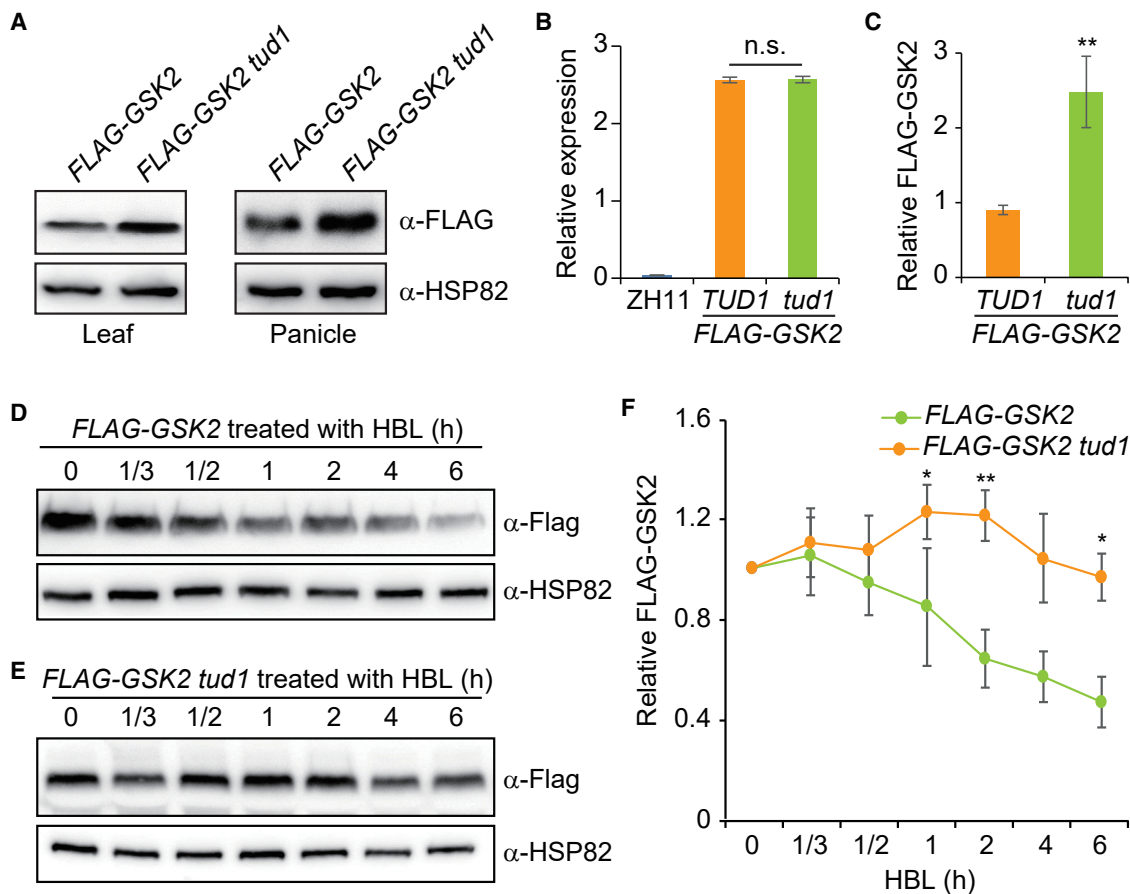


Figure 5. TUD1 mediates BR-induced GSK2 degradation in plants.

(A) Evaluation of FLAG-GSK2 in the leaf and panicle of *FLAG-GSK2* and *FLAG-GSK2 tud1*. HSP82 was detected as a control.

(B) Transcript levels of GSK2 in the two plants in (A) ($n = 3$). ZH11 was included in the analysis as a negative control. Bars indicate SD, and n.s. indicates non-significance.

(C) Statistical data for relative abundance of FLAG-GSK2 protein ($n = 3$). The values were obtained by quantification of the band strength, and those in *FLAG-GSK2* were set to 1.0. $**P < 0.01$ by *t*-test.

(D) and (E) Effect of BL treatment on GSK2 in *FLAG-GSK2* (D) and *FLAG-GSK2 tud1* (E). Plant leaves were used for the treatment by incubating with 5 μ M HBL. HSP82 was detected as a control. See Supplemental Figure 9 for more replicates as well as the mock treatment.

(F) Statistical analysis of FLAG-GSK2 abundance ($n = 3$). The values were obtained by quantification of the band strength, and those at the beginning of the treatment were set to 1.0. Bars indicate SD, and $*P < 0.05$, $**P < 0.01$ by *t*-test between the values of the two plants at the same time point.

in the wild type, whereas this process seemed much weaker or did not occur in *tud1-5* (Figure 4B and 4C). In addition, we introduced GSK2-GFP into protoplasts prepared from the wild type and *tud1-5*. Confocal microscopy observation revealed that protein fluorescence indicative of GSK2-GFP abundance was clearly stronger in the mutant than in the wild type (Supplemental Figure 6). We also introduced GFP-TUD1 or GFP alone into protoplasts prepared from *FLAG-GSK2* plants. The abundance of FLAG-GSK2 was clearly lower in the presence of GFP-TUD1 and was even lower when GFP-TUD1 expression was higher (Figure 4D). In addition, MG132 treatment was able to suppress the inhibitory effect of TUD1 on GSK2 (Figure 4E). The decreased abundance of FLAG-GSK2 in the presence of GFP-TUD1 was also supported by statistical analyses (Figure 4F). To test whether TUD1 has an effect on FLAG-GSK2, we expressed the protein in protoplasts with or without the introduction of TUD1-MYC. Although TUD1-MYC expression inhibited FLAG-GSK2 as expected, it had no effect on FLAG-

GSK2 (Supplemental Figure 7A). We further expressed FLAG-GSK2 in protoplasts isolated from either ZH11 or *tud1*, with or without TUD1-MYC. In all four samples, FLAG-GSK2 remained at a constant level (Supplemental Figure 7B). Taken together, these analyses demonstrated that TUD1 promotes GSK2 ubiquitination and degradation in response to BRs and that the mutation in aGSK2 abolishes this process.

TUD1 mediates BR-induced GSK2 degradation in plants

In order to confirm that TUD1 indeed mediates BR-induced GSK2 degradation in plants, we directly knocked out *TUD1* in *FLAG-GSK2* by CRISPR-Cas9 genome editing. A line containing a frameshift mutation in the *TUD1* coding sequence was obtained and showed typical *tud1* phenotypes (Supplemental Figure 8). In both the leaf and young panicle, we found strong accumulation of FLAG-GSK2 in the *tud1* mutant (Figure 5A). Expression analysis confirmed that GSK2 had comparable

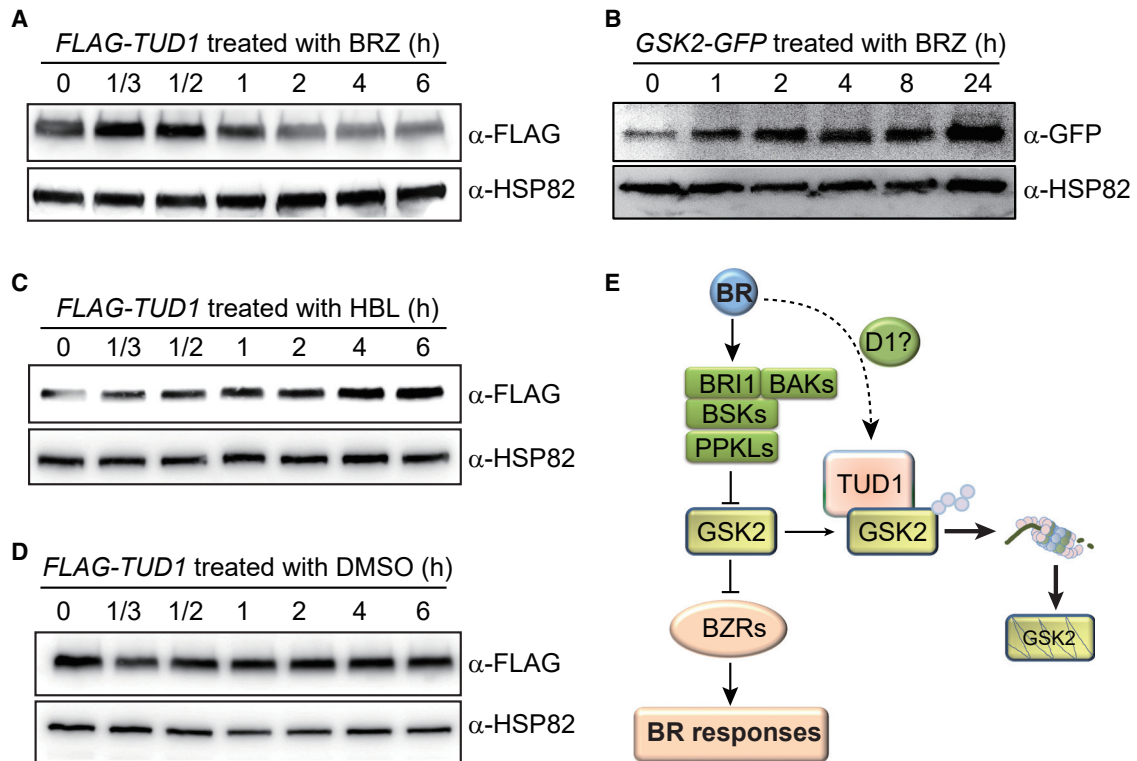


Figure 6. BRs conversely regulate TUD1 and GSK2.

(A) and (B) Effect of BRZ on TUD1 and GSK2; 10 μM BRZ was used for the treatment. HSP82 was detected as a control.

(C) Effect of BL on TUD1; 5 μM HBL was used for the treatment. HSP82 was detected as a control.

(D) Effect of mock (DMSO) treatment on TUD1, shown as a negative control.

(E) BR signaling pathway in rice, incorporating the findings of this study. TUD1 directly interacts with GSK2 and promotes GSK2 ubiquitination and degradation via the 26S proteasome. BRs also promote TUD1 accumulation, possibly via D1 (dashed line).

transcript levels in the two plants (Figure 5B). The accumulation of GSK2 in *tud1* was further confirmed in replicated assays, as shown in the statistical analysis (Figure 5C). Treatment with 28-homobrassinolide (HBL), another active BR, showed that BR-induced FLAG-GSK2 degradation was clearly delayed or impaired in the *tud1* mutant background compared with that in the wild-type *TUD1* background (Figure 5D and 5E). This result was further confirmed by replicated tests using either 1 μM HBL or 5 μM HBL for the treatment (Supplemental Figure 9A and 9B), and it was also supported by statistical analysis (Figure 5F). As a control, mock treatment with the solvent DMSO (dimethyl sulfoxide) had no effect on the protein levels (Supplemental Figure 9C). Taken together, these analyses demonstrated that TUD1 mediates BR-induced GSK2 degradation in plants.

BRs conversely regulate TUD1 and GSK2

Our results demonstrated that TUD1 promotes BR signaling via GSK2 degradation. Next, we wondered how TUD1 is regulated by BRs. At the transcriptional level, *TUD1* expression was gradually induced by treatment with BR, but not BRZ, as evaluated by real-time quantitative PCR (RT-qPCR) analysis (Supplemental Figure 10). To evaluate regulation at the protein level, we generated a number of *FLAG-TUD1*-overexpressing plants using the cauliflower mosaic virus 35S promoter. Surprisingly,

we obtained a few lines that showed decreased plant height and reduced grain size (Supplemental Figure 11A and 11B). Molecular analysis revealed that *TUD1* was highly expressed in these lines at the transcriptional level (Supplemental Figure 11C). Although the detailed reason remains unclear, the unexpected phenotypes might be attributed to over-accumulation of FLAG-TUD1 proteins (Supplemental Figure 11D). Nevertheless, these plants could be used to evaluate how BRs regulate TUD1 protein abundance. When the plants were treated with BRZ, FLAG-TUD1 was strongly suppressed (Figure 6A). By contrast, the same treatment of *GSK2-GFP*-overexpressing plants led to strong accumulation of GSK2-GFP (Figure 6B). When the plants were treated with HBL, FLAG-TUD1 was markedly induced (Figure 6C). As a control, mock treatment with DMSO had basically no effect on the protein (Figure 6D).

We tried to test whether BR treatment enhances the TUD1-GSK2 interaction using a split-luciferase complementation assay (Supplemental Figure 12A). Because aGSK2 is not responsive to BR, a test using aGSK2 was also included (Supplemental Figure 12B). Although the interaction strength between TUD1 and GSK2 appeared to decrease following BR treatment (Supplemental Figure 12C), immunoblotting analysis revealed that this decrease could be attributed to the degradation of GSK2 induced by BR (Supplemental Figure 12D). By contrast,

BR treatment clearly enhanced the TUD1-aGSK2 interaction, with no clear alteration in protein levels detected (Supplemental Figure 12B–12D). These analyses further supported our conclusion that BRs promote TUD1-mediated GSK2 degradation.

DISCUSSION

Our study demonstrated that TUD1 is involved in GSK2 ubiquitination and degradation. We provided solid evidence that GSK2 abundance is negatively associated with TUD1 in both transient and stable systems. We also showed that BR-induced GSK2 degradation is largely delayed or compromised in the absence of TUD1. Hormones are powerful substances with high activity in the regulation of cell development. Thus, plant cells in turn must develop subtle systems to control hormone responses. De-repression represents a typical hormone control mechanism that exists in most, if not all, hormonal signaling pathways. GSK2 is one of the central negative regulators of BR signaling. It appears that BRs induce TUD1 at both transcriptional and post-transcriptional levels and further promote the TUD1-GSK2 interaction in order to promptly degrade GSK2. The establishment of TUD1 as the GSK2 degradation player thus has great significance for understanding BR signaling in rice (Figure 6E).

Interestingly, TUD1 is a U-box ubiquitin ligase, whereas the KIB1 responsible for BIN2 degradation is an F-box ubiquitin ligase (Zhu et al., 2017). Sequence alignment analysis revealed that the three closest rice orthologs of KIB1 (LOC_Os03g40370, LOC_Os03g40410, LOC_Os04g08510) all showed very low similarities to KIB1, with at most 18.5% identity (Supplemental Figure 13). By contrast, the two closest *Arabidopsis* orthologs of TUD1 (AT3G49810/PUB30, AT5G65920/PUB31) showed high similarities to TUD1, with 58.4% and 55.8% identity, respectively, and PUB30, but not PUB31, can interact with BIN2 in yeast (Supplemental Figure 14). These analyses suggested that PUB30 might be involved in BIN2 degradation and that BRs could have mostly conserved but somewhat divergent signaling components in different species.

TUD1/ELF1/DSG1/D1352 has previously been reported by at least four different groups (Hu et al., 2013; Sakamoto et al., 2013; Ren et al., 2014; Wang et al., 2017). Although all these studies have demonstrated the involvement of TUD1 in BR signaling, two of them suggested that TUD1 could act in an OsBRI1-independent BR signaling pathway (Hu et al., 2013; Sakamoto et al., 2013). One of them suggested that TUD1 may interact with D1, a G protein subunit, to regulate BR signaling (Hu et al., 2013). The existence of this alternative pathway, namely the D1-TUD1 pathway, was also indicated in one of our previous reports (Tong et al., 2014). However, solid evidence is still lacking, and the relationship between OsBRI1 and D1 in BR signaling remains unclear. It should also be mentioned that there are some conflicts regarding the cytological analysis of the gene mutant. Whereas one study suggested that TUD1 promotes cell division (Hu et al., 2013), two other studies suggested that TUD1 could also regulate cell expansion (Ren et al., 2014; Wang et al., 2017). These differences may reflect the observation of different tissues at different developmental stages using different alleles. Our comparative analysis of the same tissues at the same stages revealed that TUD1 indeed

regulates cell length as GSK2 does. On the basis of our findings and previous reports, it is highly possible that both TUD1 and GSK2 regulate both cell division and cell expansion. The TUD1-GSK2 module may represent a major hub that integrates the OsBRI1- and D1-mediated BR signaling pathways, and BRs may induce TUD1 via D1 to regulate GSK2 stability (Figure 6E).

BRs regulate many important agronomic traits in crops. However, our understanding of BR signaling in crops has progressed slowly. Despite the near-completeness of the BR signaling pathway in *Arabidopsis*, many studies have suggested that BRs may have divergent signaling components, additional signaling systems, or different functions in rice (Tong and Chu, 2018). Such differences are also supported by this study. BIN2 and its family members are degraded by KIB1-family members (Zhu et al., 2017), whereas TUD1 appears to interact strongly only with GSK2. In addition, the *tud1* single mutant showed severe, typical BR-deficient phenotypes, whereas only co-suppression of three *KIB1*-homologs led to similarly severe phenotypes in *Arabidopsis* (Zhu et al., 2017). Our study thus represents a critical step forward in understanding BR signaling in a crop plant.

METHODS

Plant materials and growth conditions

Unless otherwise indicated, ZH11 was used as the wild type for transgenic, hormone treatment, and gene expression analyses. Generation of *GSK2*- and *OsBZR1*-related plants, including *FLAG-GSK2*, *FLAG-aGSK2*, *Go*, and *GFP-Myc-OsBZR1*, has been described in our previous studies (Tong et al., 2012; Liu et al., 2021). The *tud1-5* mutant was requested from and has been described previously by others (Hu et al., 2013). The *tud1* mutants in the ZH11 and *FLAG-GSK2* backgrounds were generated by editing the target sequence 5'-GCGAGAGCGC CAACATCTCG-3' using a CRISPR-Cas9 system that has been described previously (Lu et al., 2017). The coding sequence of *TUD1* was introduced into the empty binary vector 1300-35S-*FLAG* to generate *FLAG-TUD1* transgenic plants. Transgenic rice plants were generated by *Agrobacterium*-mediated transformation of rice callus. Primers used for the creation of constructs are listed in Supplemental Table 1. All rice plants were grown in the field under natural conditions or in a growth chamber on half-strength Murashige and Skoog nutrient solution (1/2 MS) at 30°C for 10 h (day/light) and at 28°C for 14 h (night/dark).

Chemical treatment, protoplast manipulation, and protein analysis

For analysis of *FLAG-GSK2*, *FLAG-aGSK2*, or *FLAG-TUD1*, 1-week-old transgenic seedlings were transferred to 1/2 MS solution supplemented with different chemicals or their combinations and cultured for different times. One micromolar BL or HBL, 5 μM HBL, or 1 μM other hormones, including GA (gibberellic acid), ACC (1-aminocyclopropane-1-carboxylic acid), ABA (abscisic acid), 6-BA (6-benzylaminopurine), KT (kinetin), IAA (indole-3-acetic acid), and JA (jasmonic acid), was used for the treatments (6 h). For BRZ and MG132, 10 μM and 20 μM were used, respectively. For analysis of *FLAG-GSK2* stability in callus, the transfected callus was prepared via *Agrobacterium*-mediated

transformation. The vector expressing FLAG-GSK2 for transfection has been detailed previously, and positive callus screened on hygromycin B was incubated with 1 μ M BL for different times. For protein analysis in protoplasts, protoplasts were prepared and transfected according to a previous method (Zhang et al., 2011). The vectors expressing GSK2-GFP have also been detailed (Tong et al., 2012), and the vector expressing GFP-TUD1 as well as TDU1-MYC was constructed in the same way using the full-length coding sequence of *TUD1*. Primers for vector construction are listed in Supplemental Table 1. After culture at 28°C overnight, the transfected protoplasts were treated with BL plus MG132 for 1 h. To test the effect of TUD1 on OsBZR1, protoplasts were isolated from *GFP-Myc-OsBZR1* and transformed with FLAG-TUD1 or empty FLAG vector. Flag leaves of *FLAG-GSK2* and *FLAG-GSK2 tud1* grown in the field at the booting stage were cut into 0.5-cm lengths and immersed in water with 5 μ M HBL and 0.2% Tween 20 for different times. The same amount of DMSO was included for the treatment as a negative control. To analyze the effect of BL on the interaction between GSK2/aGSK2 and TUD1, CLuc-GSK2 and CLuc-aGSK2 were co-infiltrated with TUD1-NLuc into *N. benthamiana* leaves. DMSO and 10 μ M HBL were injected into each side of the leaves at 6 h prior to signal detection. All the treated materials were ground into powder in liquid nitrogen, and the proteins were isolated using 2 \times SDS denaturing buffer (3 μ L/mg). The samples were boiled for 10 min and centrifuged, and the supernatants were resolved by SDS-PAGE. Proteins were detected using anti-FLAG (1:1000, Sigma), anti-GFP (1:1000, Abmart), anti-MYC (1:1000, MBL), anti-NLuc (1:1000, Sigma), anti-CLuc (1:1000, Sigma), and anti-HPT (1:1000, BPI) antibodies. Blotting against the heat shock protein HSP82 (1:2000, BPI) or staining using Ponceau S was included as a reference.

Protein–protein interaction

Vectors for all the following analyses were constructed by introducing the full-length coding sequences of the genes into empty vectors using the in-fusion strategy. Also, see our previous studies for the available vectors related to GSK2 and aGSK2 (Liu et al., 2021; Tong et al., 2012). All primers and resulting vectors are listed in Supplemental Table 1. A yeast two-hybrid assay was performed using the Matchmaker Gold Yeast Two-Hybrid System (Clontech) according to the product instructions. The pull-down assay and expression and purification of fusion proteins were performed as described previously (Liu et al., 2022). BiFC, luciferase complementation, and Co-IP assays were performed as detailed previously (Chen et al., 2008; Xiao et al., 2020; Liu et al., 2022). The fluorescence was detected with a confocal fluorescence microscope (LSM 980, ZEISS). The luminance signal was detected with an imaging system equipped with a cold charge-coupled device camera (LB 985, NightSHADE with indiGO software). Detection of proteins by immunoblotting was performed using tag antibodies including anti-FLAG (1:1000, Sigma), anti-GFP (1:1000, Abmart), anti-GST (1:2000, Abmart), and anti-MBP (1:2000, Abmart).

Microscopy observation

The third leaf sheaths of 1-month-old seedlings were used to prepare longitudinal sections for comparison of cell length as described previously (Hu et al., 2013). The middle part with ~1-cm length of the sheath was decolorized with ethanol and then

immersed in water for observation under a light microscope (BX53, Olympus). Whole grains with husks were treated as previously described (Jin et al., 2011) for observation of the epidermal cells of the lemma under a scanning electron microscope (S-3000N, Hitachi). Cell length was quantified using ImageJ software.

In vitro ubiquitination assay

The *in vitro* ubiquitination was carried out as detailed previously (Yu et al., 2020), and the purified proteins used for analysis, including His-Ub, His-E1 (wheat, GI:136632), and His-E2 (human, UBCh5B), have been described. In brief, GST-GSK2 and MBP-TUD1 were mixed with His-Ub, His-E1, and His-E2 in the reaction buffer (50 mM Tris-HCl, pH 7.5, 2 mM ATP, 5 mM MgCl₂, 2 mM DTT). The mixture with different combinations of the proteins was incubated at 30°C for 90 min, and SDS sample buffer was added to stop the reaction. The samples were boiled for 5 min and separated by SDS-PAGE. An immunoblotting assay was performed with anti-GST antibody (1:2000, Abmart) to detect the ubiquitination of GST-GSK2.

RNA sequencing

For RNA sequencing, 10-day-old seedlings of *Go-3*, *tud1*, and their background material ZH11 were grown in a greenhouse and used for extraction of total RNA. At least 15 seedlings were pooled for each sample. Library construction and Illumina sequencing were performed by Biomarker Technologies. False discovery rate or P value < 0.05 and absolute value of log₂(fold change) \geq 1.5 were used to identify DEGs. The three BR biosynthesis genes and three signaling genes used to draw the heat map were selected according to the KEGG (Kyoto Encyclopedia of Genes and Genomes) annotation. Both data analysis and visualization of the Venn diagram, heat map, and common expression patterns were performed using BMKCloud (www.biocloud.net).

RT-qPCR

Total RNA was extracted from 1-week-old seedlings using TRIzol Reagent (Invitrogen). Synthesis of cDNA was performed with 2 μ g total RNA using ReverTra Ace qPCR RT Master Mix (Toyobo), and RT-qPCR was performed in 96-well plates using FastStart Essential DNA Green Master (Roche) on a real-time PCR detection system (Roche LightCycler 96). Rice *ACTIN1* was used as the reference. Primer sequences are listed in Supplemental Table 2.

ACCESSION NUMBERS

Sequence data from this article can be found at the Rice Genome Project website (<http://rice.plantbiology.msu.edu/>) under the accession numbers LOC_Os03g13010 (*TUD1*), LOC_Os01g10840 (*GSK1*), LOC_Os05g11730 (*GSK2*), LOC_Os02g14130 (*GSK3*), LOC_Os06g35530 (*GSK4*), LOC_Os03g40370, LOC_Os03g40410, and LOC_Os04g08510 or at the Arabidopsis Information Resource website (<https://www.arabidopsis.org/>) under the accession numbers AT1G67160 (*KIB1*), AT3G49810 (*PUB30*), and AT5G65920 (*PUB31*). The RNA sequencing data in this study have been deposited at the National Genomics Data Center (<http://ngdc.cncb.ac.cn/gsa/>) under the accession number CRA008101.

SUPPLEMENTAL INFORMATION

Supplemental information is available at *Plant Communications Online*.

FUNDING

This work was supported by the Hainan Yazhou Bay Seed Laboratory (B21HJ0215), the National Natural Science Foundation of China (nos. U21A20208, 31900177, 31901534, 31871587), and the Central Public-interest Scientific Institution Basal Research Fund (no. S2022ZD02). D.L. was funded by the China Postdoctoral Science Foundation (2020M670548).

AUTHOR CONTRIBUTIONS

H.T. conceived and designed the study. D.L. and X.Z. conducted the experiments. Q.L., Y.X., G.Z., W.Y., M.N., W.M., N.D., J.L., Y.Y., and H.T. provided assistance. D.L. and H.T. analyzed the data and wrote the article. H.T., C.C., and Q.X. discussed the data and co-supervised the study.

ACKNOWLEDGMENTS

We thank Prof. Yongbiao Xue (Institute of Genetics and Developmental Biology, Chinese Academy of Sciences) and Dr. Xinming Hu (Anhui Agricultural University) for providing the *tud1-5* mutant. The authors declare no conflict of interest.

Received: December 29, 2021
 Revised: June 28, 2022
 Accepted: September 9, 2022
 Published: September 20, 2022

REFERENCES

- Bai, M.Y., Zhang, L.Y., Gampala, S.S., Zhu, S.W., Song, W.Y., Chong, K., and Wang, Z.Y. (2007). Functions of OsBZR1 and 14-3-3 proteins in brassinosteroid signaling in rice. *Proc. Natl. Acad. Sci. USA* **104**:13839–13844.
- Chen, H., Zou, Y., Shang, Y., Lin, H., Wang, Y., Cai, R., Tang, X., and Zhou, J.M. (2008). Firefly luciferase complementation imaging assay for protein–protein interactions in plants. *Plant Physiol.* **146**:368–376.
- Grove, M.D., Spencer, G.F., Rohwedder, W.K., Mandava, N., Worley, J.F., Warthen, J.D., Steffens, G.L., Flippen-Anderson, J.L., and Cook, J.C. (1979). Brassinolide, a plant growth-promoting steroid isolated from *Brassica napus* pollen. *Nature* **281**:216–217.
- He, J.X., Gendron, J.M., Yang, Y., Li, J., and Wang, Z.Y. (2002). The GSK3-like kinase BIN2 phosphorylates and destabilizes BZR1, a positive regulator of the brassinosteroid signaling pathway in *Arabidopsis*. *Proc. Natl. Acad. Sci. USA* **99**:10185–10190.
- Hu, X.M., Qian, Q., Xu, T., Zhang, Y., Dong, G., Gao, T., Xie, Q., and Xue, Y. (2013). The U-box E3 ubiquitin ligase TUD1 functions with a heterotrimeric G alpha subunit to regulate brassinosteroid-mediated growth in rice. *PLoS Genet.* **9**:e1003391.
- Jin, Y., Luo, Q., Tong, H., Wang, A., Cheng, Z., Tang, J., Li, D., Zhao, X., Li, X., Wan, J., et al. (2011). An AT-hook gene is required for palea formation and floral organ number control in rice. *Dev. Biol.* **359**:277–288.
- Kim, T.W., Guan, S., Burlingame, A.L., and Wang, Z.Y. (2011). The CDG1 kinase mediates brassinosteroid signal transduction from BRI1 receptor kinase to BSU1 phosphatase and GSK3-like kinase BIN2. *Mol. Cell* **43**:561–571.
- Li, D., Wang, L., Wang, M., Xu, Y.Y., Luo, W., Liu, Y.J., Xu, Z.H., Li, J., and Chong, K. (2009). Engineering *OsBAK1* gene as a molecular tool to improve rice architecture for high yield. *Plant Biotechnol. J.* **7**:791–806.
- Li, J., Wen, J., Lease, K.A., Doke, J.T., Tax, F.E., and Walker, J.C. (2002). BAK1, an *Arabidopsis* LRR receptor-like protein kinase, interacts with BRI1 and modulates brassinosteroid signaling. *Cell* **110**:213–222.
- Li, J.M., and Nam, K.H. (2002). Regulation of brassinosteroid signaling by a GSK3/SHAGGY-like kinase. *Science* **295**:1299–1301.
- Liu, D., Yu, Z., Zhang, G., Yin, W., Li, L., Niu, M., Meng, W., Zhang, X., Dong, N., Liu, J., et al. (2021). Diversification of plant agronomic traits by genome editing of brassinosteroid signaling family genes in rice. *Plant Physiol.* **187**:2563–2576.
- Liu, D., Zhao, H., Xiao, Y., Zhang, G., Cao, S., Yin, W., Qian, Y., Yin, Y., Zhang, J., Chen, S., et al. (2022). A cryptic inhibitor of cytokinin phosphorelay controls rice grain size. *Mol. Plant* **15**:293–307.
- Lu, Y.M., Ye, X., Guo, R., Huang, J., Wang, W., Tang, J., Tan, L., Zhu, J.K., Chu, C., and Qian, Y. (2017). Genome-wide targeted mutagenesis in rice using the CRISPR/Cas9 system. *Mol. Plant* **10**:1242–1245.
- Mora-Garcia, S., Vert, G., Yin, Y., Caño-Delgado, A., Cheong, H., and Chory, J. (2004). Nuclear protein phosphatases with Kelch-repeat domains modulate the response to brassinosteroids in *Arabidopsis*. *Genes Dev.* **18**:448–460.
- Nam, K.H., and Li, J. (2002). BRI1/BAK1, a receptor kinase pair mediating brassinosteroid signaling. *Cell* **110**:203–212.
- Nolan, T.M., Vukasinić, N., Liu, D., Russinova, E., and Yin, Y. (2020). Brassinosteroids: multidimensional regulators of plant growth, development, and stress responses. *Plant Cell* **32**:295–318.
- Peng, P., Yan, Z., Zhu, Y., and Li, J. (2008). Regulation of the *Arabidopsis* GSK3-like kinase BRASSINOSTEROID-INSENSITIVE 2 through proteasome-mediated protein degradation. *Mol. Plant* **1**:338–346.
- Ren, Y., Tang, Y., Xie, K., Li, W., Ye, S., Gao, F., Zou, T., Li, X., Deng, Q., Wang, S., et al. (2014). Mutation of a U-box E3 ubiquitin ligase results in brassinosteroid insensitivity in rice. *Mol. Breeding* **34**:115–125.
- Sakamoto, T., Kitano, H., and Fujioka, S. (2013). An E3 ubiquitin ligase, ERECT LEAF1, functions in brassinosteroid signaling of rice. *Plant Signal. Behav.* **8**:e27117.
- Tang, W.Q., Kim, T.W., Osés-Prieto, J.A., Sun, Y., Deng, Z., Zhu, S., Wang, R., Burlingame, A.L., and Wang, Z.Y. (2008). BSKs mediate signal transduction from the receptor kinase BRI1 in *Arabidopsis*. *Science* **321**:557–560.
- Tang, W.Q., Yuan, M., Wang, R.J., Yang, Y.H., Wang, C.M., Osés-Prieto, J.A., Kim, T.W., Zhou, H.W., Deng, Z.P., Gampala, S.S., et al. (2011). PP2A activates brassinosteroid-responsive gene expression and plant growth by dephosphorylating BZR1. *Nat. Cell Biol.* **13**:124–131.
- Tong, H., and Chu, C. (2018). Functional specificities of brassinosteroid and potential utilization for crop improvement. *Trends Plant Sci.* **23**:1016–1028.
- Tong, H., Xiao, Y., Liu, D., Gao, S., Liu, L., Yin, Y., Jin, Y., Qian, Q., and Chu, C. (2014). Brassinosteroid regulates cell elongation by modulating gibberellin metabolism in rice. *Plant Cell* **26**:4376–4393.
- Tong, H., Liu, L., Jin, Y., Du, L., Yin, Y., Qian, Q., Zhu, L., and Chu, C. (2012). DWARF AND LOW-TILLERING acts as a direct downstream target of a GSK3/SHAGGY-like kinase to mediate brassinosteroid responses in rice. *Plant Cell* **24**:2562–2577.
- Wang, N., Xing, Y., Lou, Q., Feng, P., Liu, S., Zhu, M., Yin, W., Fang, S., Lin, Y., Zhang, T., et al. (2017). *Dwarf and short grain 1*, encoding a putative U-box protein regulates cell division and elongation in rice. *J. Plant Physiol.* **209**:84–94.
- Wang, Z.Y., Seto, H., Fujioka, S., Yoshida, S., and Chory, J. (2001). BRI1 is a critical component of a plasma-membrane receptor for plant steroids. *Nature* **410**:380–383.
- Wu, G., Wang, X., Li, X., Kamiya, Y., Otegui, M.S., and Chory, J. (2011). Methylation of a phosphatase specifies dephosphorylation and degradation of activated brassinosteroid receptors. *Sci. Signal.* **4**:ra29.
- Xiao, Y., Zhang, G., Liu, D., Niu, M., Tong, H., and Chu, C. (2020). GSK2 stabilizes OFP3 to suppress brassinosteroid responses in rice. *Plant J.* **102**:1187–1201.

- Yamamuro, C., Ihara, Y., Wu, X., Noguchi, T., Fujioka, S., Takatsuto, S., Ashikari, M., Kitano, H., and Matsuoka, M.** (2000). Loss of function of a rice *brassinosteroid insensitive1* homolog prevents internode elongation and bending of the lamina joint. *Plant Cell* **12**:1591–1606.
- Yin, Y., Wang, Z.Y., Mora-Garcia, S., Li, J., Yoshida, S., Asami, T., and Chory, J.** (2002). BES1 accumulates in the nucleus in response to brassinosteroids to regulate gene expression and promote stem elongation. *Cell* **109**:181–191.
- Yu, F., Cao, X., Liu, G., Wang, Q., Xia, R., Zhang, X., and Xie, Q.** (2020). ESCRT-I component VPS23A is targeted by E3 ubiquitin ligase XBAT35 for proteasome-mediated degradation in modulating ABA signaling. *Mol. Plant* **13**:1556–1569.
- Zhang, B., Wang, X., Zhao, Z., Wang, R., Huang, X., Zhu, Y., Yuan, L., Wang, Y., Xu, X., Burlingame, A.L., et al.** (2015). OsBRI1 activates BR signaling by preventing binding between the TPR and kinase domains of OsBSK3 via phosphorylation. *Plant Physiol.* **170**:1149–1161.
- Zhang, Y., Su, J., Duan, S., Ao, Y., Dai, J., Liu, J., Wang, P., Li, Y., Liu, B., Feng, D., et al.** (2011). A highly efficient rice green tissue protoplast system for transient gene expression and studying light/chloroplast-related processes. *Plant Methods* **7**:30.
- Zhu, J.Y., Li, Y., Cao, D.M., Yang, H., Oh, E., Bi, Y., Zhu, S., and Wang, Z.Y.** (2017). The F-box protein KIB1 mediates brassinosteroid-induced inactivation and degradation of GSK3-like kinases in *Arabidopsis*. *Mol. Cell* **66**:648–657.e4.